Model based on trap-assisted tunneling for two-level current fluctuations in submicrometer metal–silicon-dioxide–silicon diodes

M. O. Andersson, Z. Xiao, S. Norrman, and O. Engström
Department of Solid State Electronics, Chalmers University of Technology, S-412 96 Göteborg, Sweden
(Received 29 December 1989)

A new model is suggested to explain the characteristics of discrete two-level current fluctuations (TLF's) in metal–silicon-dioxide–silicon tunnel diodes. The model is based on trap-assisted tunneling via a single-electron trap. The trap does not act merely as a point charge in the oxide, but can function as an intermediate state for electrons that tunnel from the metal to the silicon. We show that this model can explain the large fluctuation amplitudes, and we use an atomic relaxation effect to account for the thermally activated capture and emission time constants found in our measurements. Because of the relative simplicity of the model, quantitative comparisons with experiments are possible.

I. INTRODUCTION

When electric currents are forced through volumes of submicrometer dimensions, two-level current fluctuations (TLF's) have been found in a number of materials and structures. The phenomenon has been observed in the gate channel regions of metal–silicon-dioxide–silicon (MOS) field-effect transistors[1–3] and in junction field-effect transistors (JFET's).[4] For the former devices, an extensive review has recently been published by Kirton and Uren.[5] Also for tunnel structures of MOS type and for metal-insulator-metal (MIM) structures, similar phenomena have been observed in a number of cases.[6–9] For this geometry, where the current passes perpendicularly to the insulator layer, no detailed model has yet been developed to explain all measured characteristics. The phenomenon is clearly of great complexity, and the limited number of measurables makes the synthesis of such a model a difficult task.

The simplest way to explain the occurrence of TLF's in MIM and MOS structures would be to assume a single electron trap located in the insulator between the electrodes. When the trap is occupied, the current is low. For the case that the trap becomes positively charged on ionization, its attractive potential lowers the tunnel barrier very locally. The major problem with this model is that the largest possible magnitude of the fluctuation would be a factor of about 5×10^{-5} of the dc level.[10] Such a small modulation could not be resolved in our measurements, and we have measured modulations up to 200 pA or 30% of the current.

This leaves at least two possibilities: either some other mechanism, much more efficient than simple Coulombic attraction, has to be assumed to explain the dramatic changes in conductivity, or else a number of these traps have to change their configuration or charge contents simultaneously. A model for the latter case, based on the existence of correlated multielectron processes, has been proposed.[8] To our understanding, this model introduces a new physical principle in the sense that electrons can be captured and emitted *collectively* in a defect reconfiguration. We feel that such an approach is unsatisfactory due to the lack of detailed data supporting this new phenomenon.

We suggest a model based on trap-assisted electron tunneling via a *single* trap to explain our measured data on MOS tunnel diodes. The trap does not act merely as a point charge in the oxide, but can function as an intermediate state for electrons that tunnel from the metal to the silicon. This model can explain the large fluctuation amplitudes, and a detailed calculation for a specific example is presented. The model uses an atomic relaxation effect to account for the thermally activated capture and emission time constants found in our measurements. So, the current enhancement mechanism consists of a combination of well established physical processes and involves only a few adjustable parameters. We deal merely with "native" effects as opposed to wear-out effects induced by high fields or large currents for long times.

II. EXPERIMENTAL DETAILS

The diodes used in our measurements were made on a p-type silicon wafer with ⟨100⟩ surface orientation, and the gate oxides were grown in dry oxygen at about 700 °C to a thickness of about 25 Å. A 1000-Å field oxide surrounds the active gate, which typically has a diameter of 0.4 μm, masked using an e-beam technique. Aluminum was evaporated both as gate metal in squares of 250 by 250 μm covering the small gates, and as backside contacts with very good Ohmic characteristics.

Figure 1 shows the experimental setup. The measurement procedure begins by searching for a TLF which seems to have a steady state and a large enough amplitude. Components showing more complex time traces, which may be due to the presence of more than one trap, were rejected in this study. Having found a suitable component, its dc I-V curve is recorded using the electrometer. The bias is changed very slowly in small steps to avoid measuring displacement currents, and the tempera-

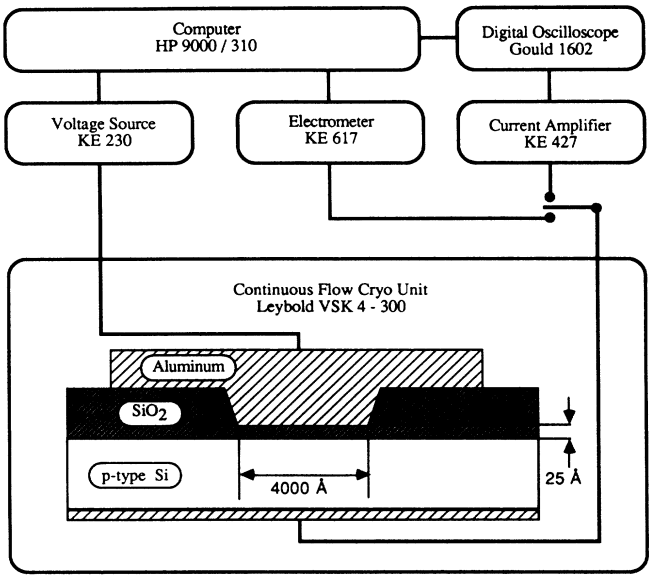

FIG. 1. Schematic picture of the computer-controlled measurement setup and the diode structure.

ture is kept at 100 K during the *I-V* characterization to reduce the influence of thermal effects on the tunnel current[11] and to inhibit the fluctuations. At the decided gate voltage and temperature, the current amplifier and digital oscilloscope sample 30 720 points of the fluctuation time trace, which are transferred to the computer and stored. A part of such a trace is shown in Fig. 2, where the mean times in the high- and low-current states are denoted τ_c and τ_e, respectively. The trace duration is adjusted so as to gather a minimum of 50 fluctuations per trace, but more often 100 to 200. A tradeoff has to be made between the number of fluctuations collected and the density of samples so that a sufficient number of measurement points are collected in each fluctuation. Except when the TLF magnitude is measured (prior to the time trace), the step rise time of the current amplifier is adjust-

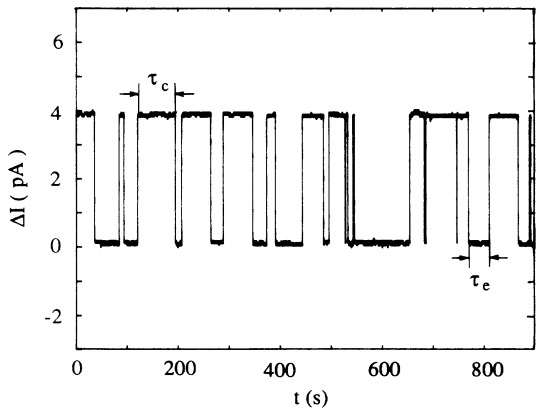

FIG. 2. Measured current fluctuation at a gate voltage of −2.2 V and a temperature of 110 K for the component analyzed in this paper. The dc level, not shown in the figure, was 44 pA. The times denoted τ_c and τ_e are the mean times in the high-current and low-current modes, respectively.

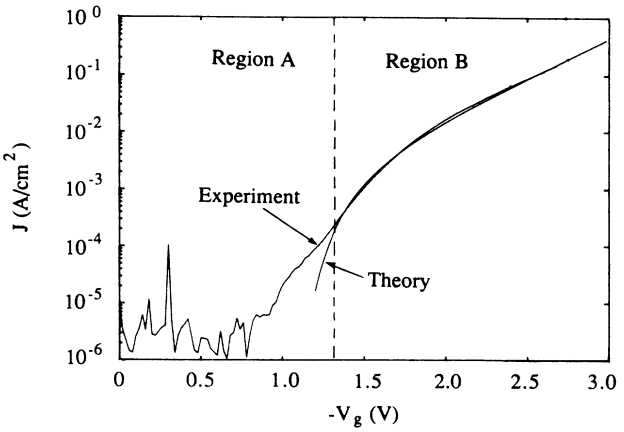

FIG. 3. Measured and theoretically fitted current density vs the negative of the gate voltage. The two regions shown are explained in the text. The theoretical fit was obtained using a value of 22.5 Å for the oxide thickness. The temperature was 100 K.

ed so as to minimize the error made in determining the mean times in the low- and high-current states, rather than to minimize the inherent high-frequency system noise. The latter has no influence on the statistics of the TLF's, as long as its amplitude is substantially smaller than the fluctuation amplitude and thus the risk of false counts is minimized.

A computer routine determines the mean times τ_c and τ_e using an artificial trigger value, e.g., 2 pA in Fig. 2. A new bias or temperature is chosen and the collection procedure is repeated. In this manner, the bias-temperature plane is swept either until the practical limits of the time constants are reached or, more frequently, until the TLF is spontaneously deactivated.

III. EXPERIMENTAL RESULTS

A majority of our diodes exhibit a current density versus gate voltage dependence as shown in Fig. 3 (the experimental line) for the component we focus on this paper. As will be justified in Sec. IV A, the concentrations of oxide fixed charge and interface state charge are as-

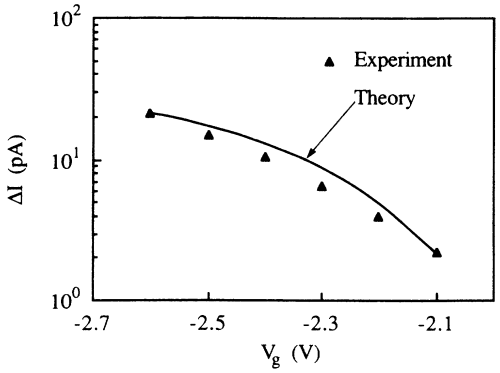

FIG. 4. Measured and theoretically fitted fluctuation amplitude vs gate voltage. The amplitude varied less than 5% as the temperature was increased from 100 to 150 K.

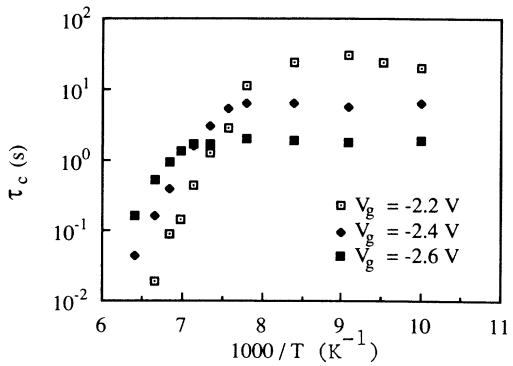

FIG. 5. Measured capture time constant vs inverse temperature at three gate voltages.

sumed to be negligible. Then, at zero bias, the silicon surface is in inversion due to our choice of gate metal.[12] A gate voltage of about -1.1 V has to be applied to reach the flatband condition. Generally, the TLF's occurring in our components have been found in the bias interval $-2.6\ \text{V} \le V_g \le -1.3$ V, denoted "Region B" in Fig. 3, where V_g is the applied gate voltage. This means that the silicon surface is in accumulation during the characterization of a TLF.[12] The current that would normally appear for $-1.0\ \text{V} \le V_g$ in the semiconductor limited current region,[12] denoted "Region A" in Fig. 3, is negligible here due to the small gate area and to the low temperature. The apparent current in Fig. 3 for these voltages is actually noise.

As shown in Fig. 4, the current fluctuation amplitude ΔI varies approximately exponentially with applied bias. In contrast, the temperature dependence of ΔI is very weak; no variation could be detected as the temperature was increased from 100 to 150 K, which means that the change was less than 5%. Figure 5 shows that at higher temperatures, τ_c is thermally activated with an activation energy ΔE_c, but exhibits a pronounced saturation at lower temperatures. The voltage dependences are also inverted as the curves cross at about 130 K. On the other hand, τ_e shows a nearly exponential dependence on both temperature and bias as shown in Fig. 6.

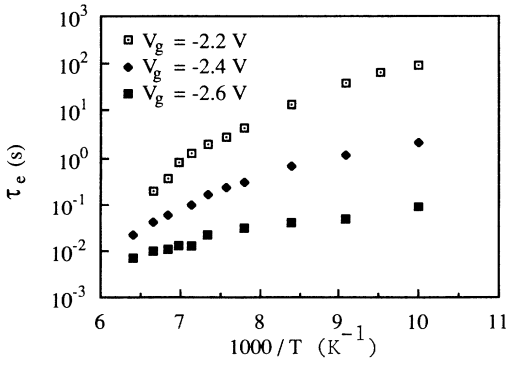

FIG. 6. Measured emission time constant vs inverse temperature at three gate voltages.

IV. THEORY

In the following subsections, the primary objectives are to explain the large TLF amplitude and its bias dependence together with the complicated dependences of τ_c and τ_e on bias and temperature. Prior to presenting the model, we will verify that our components exhibit overall current-voltage characteristics as expected from the type of diodes used in the investigation.

A. The current-voltage relationship of the background tunnel current

The dc background current is dominated by direct electron tunneling from states below the metal Fermi level through the thin oxide to states in the Si conduction band.[12] The expression used for the current density in the tunnel-limited voltage region ("region B") is[13]

$$J=\frac{4\pi q m_{\text{Al}}}{h^3}\int_0^{E_{F,m}} D(E)E\,dE\ , \tag{1}$$

where q is the magnitude of the electron charge, h is Planck's constant, the effective electron mass in aluminum m_{Al} is taken as $1.2m_0$, where the latter denotes the free-electron mass, E is the total energy above the silicon conduction-band edge, and $E_{F,m}$ is the metal Fermi level. In the WKB approximation we have[13]

$$D(E)=\exp\left[-2\int_0^{t_{\text{ox}}}\kappa(x)dx\right]\ . \tag{2}$$

Here, x is the distance from the metal-oxide interface, t_{ox} is the oxide thickness, and $\kappa(x)$ is the imaginary part of the wave vector in the oxide. The latter is expressed as

$$\kappa(x)=\frac{2\pi}{h}[2m_{\text{ox}}\,\Delta E(x)]^{1/2}\ , \tag{3}$$

where $\Delta E(x)$, is the energy difference between the trapezoidal oxide barrier at point x and the energy of the tunneling electron. A one-band parabolic approximation for the energy-momentum relation in the oxide is used in Eq. (3). For the effective mass in the oxide we use[14] $m_{\text{ox}}=0.5m_0$. The electronic image-potential correction has deliberately been omitted, since it has been shown to be negligible.[15] Region A is of small interest in this context, and we have not included it in the analysis. The best fit is obtained using $t_{\text{ox}}=22.5$ Å, as shown in Fig. 3. This is not in conflict with the 25-Å premetalization value mentioned above, since aluminum is known to reduce the oxide thickness somewhat.

It is interesting to note the good agreement between measured and theoretical current densities in Region B. The overall fit is in contrast to the results obtained from similar diodes by Maserjian,[16] who found that the current was substantially lower than theoretically predicted at $-3.4\ \text{V} \le V_g$, whereas it approached the predicted values at more negative gate voltages. This phenomenon has been attributed to effects of tunneling to the indirect conduction band of the silicon or strain effects in the thin oxide.[13] If present, these effects should also have an influence on the voltage dependence of ΔI in our model which will be discussed in the next section.

Since the phenomenon is absent in our components, we have not tried to include such effects in the trap-assisted tunneling model. We also conclude that oxide fixed charge or interface state charge does not influence the relationship between surface potential and gate voltage to any significant degree, since no displacement in voltage of the measured *I-V* curve with respect to the theoretical curve can be detected.

B. The fluctuation amplitude

In the model, we assume that the trap ground state is located well below the conduction-band edge of the silicon and also below the Fermi level of the metal at all gate voltages, as shown in Fig. 7. The trap has an excited state which is located below the metal Fermi level, but above the silicon conduction band.

The following qualitative explanation of the model is perhaps best understood with the aid of Fig. 8. An electron which tunnels from the metal to the trap can be captured to the excited state with a time constant τ_{tc}, in which case it tunnels very rapidly out to the silicon with a time constant τ_{te}. The current is high for as long as this process continues. Alternatively, the electron may be captured to the ground state with a time constant τ_c, thereby closing the tunnel path through the excited state, and the current becomes normal (=low). From the ground state, the electron must be emitted thermally with a time constant τ_e before it can tunnel either to the Si conduction band or, alternatively, to the top of the valence band where holes are accumulated. This is a much slower process than the two-step tunneling across the excited state. After the electron emission, the trap relaxes and becomes ready to accept a new electron, which

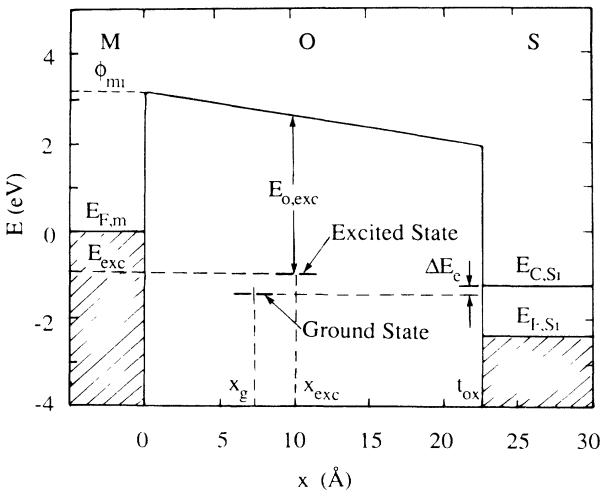

FIG. 7. Band diagram, drawn to scale, showing the positions in energy and the distances from the metal of the two bound states of the trap as deduced from the model. Also shown are the calculated barriers for tunneling to and from the excited state. The *p*-type silicon is in accumulation, and for the sake of simplicity we have let the silicon Fermi level coincide with the valence-band edge at the interface.

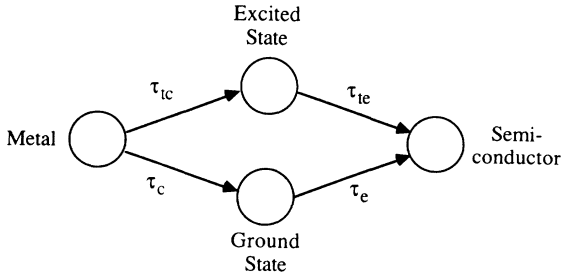

FIG. 8. The essential electron transport paths of the model, illustrated schematically.

is captured either to the ground state again or to the excited state.

The fluctuation magnitude, ΔI, is determined by the rate at which electrons tunnel from the metal to the excited state, and then on to the silicon:

$$\Delta I = \frac{q}{\tau_t} , \tag{4}$$

where q is the magnitude of the electron charge and τ_t is the total time constant for the two-step tunnel process:

$$\tau_t = \tau_{tc} + \tau_{te} . \tag{5}$$

We have found that our data fits the theory best if the trap is about 2.5 Å closer to the metal than to the silicon, as in Fig. 7. From this, using the theory as outlined below for both transitions, we find that $\tau_{te}/\tau_{tc} \approx 10$ or larger, as will be commented on below. Qualitatively, this effect occurs because the tunnel time constants increase exponentially with increasing tunnel distance. So, Eq. (4) can be approximated as

$$\Delta I = \frac{q}{\tau_{te}} . \tag{6}$$

To calculate τ_{te}, a simple potential and its corresponding wave function are assumed for the excited state. The state must be deeper in energy than about 3 eV with reference to the oxide conduction band, or it could not be filled from the metal. Electron states on such deep energy levels are normally expected to have localized electron potentials in real space. This suggests, as an approximation, the use of a three-dimensional δ potential,[17] and we can therefore directly use the result of Lundström and Svensson,[18] who calculated the tunnel time constant under these premises from first principles using a Bardeen formalism.[19] We believe that this potential can be used as an approximation of the real, tight potential also for the excited state of the trap, even if a perfect δ potential would not produce an excited state. For a more realistic potential with a finite extension, the tunnel barriers will decrease, and thus also the time constants τ_{tc} and τ_{te}. Then, to fit the measured ΔI data, the excited state must be moved closer to the metal to increase τ_{te}. However, moving the state closer to the metal will further decrease τ_{tc}, and so the ratio τ_{te}/τ_{tc} will increase above the value of 10 mentioned above. Again, the electronic image-potential correction has deliberately been omitted in cal-

culating the barrier. In fact, in turns out that even if we do include it, its influence would be to move the calculated position of the excited state approximately 1 Å closer to the metal. Also this effect would increase the ratio τ_{te}/τ_{tc} mentioned above, which in turn would improve the validity of the approximation used in Eq. (6).

In the WKB approximation we have[18]

$$\tau_{te}=\tau_{0,te}\exp\left[2\int_{x_{exc}}^{t_{ox}}\kappa(x)dx\right], \tag{7}$$

where x_{exc} denotes the position of the excited state. The imaginary part of the wave vector in the oxide, $\kappa(x)$, is expressed as[18]

$$\kappa(x)=\frac{2\pi}{h}\{2m_{ox}[\phi_t(x)-E_{exc}]\}^{1/2} \tag{8}$$

again using a one-band parabolic approximation for the energy-momentum relation in the oxide conduction band. In Eq. (8), $\phi_t(x)$ and E_{exc} are the energy barrier for tunneling and the energy position of the excited state, respectively, as measured from the metal Fermi energy. The barrier, shown in Fig. 7, can be described by

$$\phi_t(x)=\phi_{mi}-qV_{ox}\frac{x}{t_{ox}},\quad x\neq x_{exc} \tag{9}$$

where $\phi_{mi}=3.2$ eV is the metal-oxide work-function difference, and V_{ox} is the voltage across the oxide (deduced from the gate voltage V_g using standard MOS arguments assuming no other oxide or interface charges). The energy position with regard to the metal Fermi level of the excited state, as shown in Fig. 7, is described by

$$E_{exc}=\phi_{mi}+qV_{ox}\frac{x_{exc}}{t_{ox}}-E_{0,exc}, \tag{10}$$

where $E_{0,exc}$ is the energy depth of the excited state below the oxide conduction band. Finally, the preexponential factor in Eq. (7) is expressed by[18]

$$\tau_{0,te}^{-1}=\frac{8\pi h m_{Si}}{m_{ox}^2}\frac{\kappa}{\kappa^2+k_0^2}\times\int_0^{k_0}(k_0^2-k_\parallel^2)^{1/2}\times\exp\left[-\frac{k_\parallel^2(t_{ox}-x_{exc})}{\kappa}\right]k_\parallel\,dk_\parallel, \tag{11}$$

where we use $m_{Si}=1.18m_0$, κ is the mean value of $\kappa(x)$, and k_0 is the maximum value that the absolute of the y- and z-directed wave vectors, $k_\parallel$, can take:

$$k_0\equiv\frac{2\pi}{h}(2m_{Si}E_r)^{1/2}, \tag{12}$$

where

$$E_r=E_{exc}-E_{C,Si}. \tag{13}$$

$E_{C,Si}$ denotes the energy below the metal Fermi energy of the silicon conduction-band edge at the interface at a given gate voltage. The voltage dependence of ΔI is contained in Eqs. (9), (10), and (13), and consists of two cooperating contributions: (1) the change in barrier height; and (2) the change in E_r.

The free parameters to be fitted are $E_{0,exc}$ and x_{exc}. The integral in Eq. (11) is evaluated numerically. The procedure is repeated for varying V_g until we obtain a graph as shown in Fig. 4, where we used $x_{exc}=10.2$ Å and $E_{0,exc}=3.6$ eV (see also Fig. 7). The obtained position of the excited state is unique, i.e., no other combination of the two parameters could give the same voltage dependence of ΔI.

Finally, we conclude that the possibility of back tunneling from the excited state to the metal does not influence ΔI; as long as the ratio τ_{te}/τ_{tc} is large, the excited state would still be filled often enough not to affect the slower tunneling between the excited state and the silicon, which determines ΔI.

C. The time constants for charge communication with the ground state

The mean time in the high-current state, τ_c, is the time constant for electron capture from the metal to the ground state of the trap, and the mean time in the low-current state, τ_e, is the time constant for electron emission from the same ground state to the silicon. Both of these are typically much larger than the time constants discussed in the previous section, because they are not determined by elastic tunneling alone but, in addition, by a thermal activation process.

The simplest data to explain is the τ_e data, demonstrated in Fig. 6, if we for a moment disregard the weak curvature in the temperature dependence of τ_e. The exponential voltage dependence occurs because the energy position of the ground state with respect to the silicon conduction band changes linearly with the gate voltage; see Fig. 7. The temperature dependence is deduced assuming a Boltzmann distribution for the atomic vibrational modes of the ground state. In the configuration-coordinate diagram in Fig. 9, this is illustrated as the transition between the oscillator potentials denoted "A" and "C." The potential curves represent the turning points of the atomic vibrations of the trap,[20] and their positions on the energy scale reflect the electronic energy for which they are drawn. In Fig. 9, the "A" curve represents the occupied ground state of the trap, which is fixed with respect to the oxide conduction band. Curve "B" represents the ionized trap at an electronic energy equal to the Fermi level in the metal. The "C" curve is drawn for the ionized trap and with the electron at the bottom of the silicon conduction band. So, for increasingly negative gate voltage, "A" will move upwards with respect to "C," and "B" will move upwards with respect to "A." This means that the activation energy ΔE_e for transfer from "A" to "C" is expected to decrease for increasingly negative gate voltages. The time constant for emission from the ground state can be expressed as

$$\tau_e=\tau_{0,e}\exp\left[\frac{\Delta E_e}{kT}\right], \tag{14}$$

where

$$\Delta E_e=\Delta E_{0,e}-qV_g\left[1-\frac{x_g}{t_{ox}}\right] \tag{15}$$

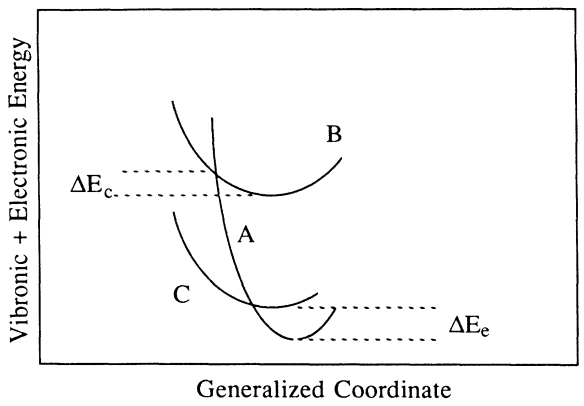

FIG. 9. A schematic configuration-coordinate diagram illustrating the occurrence of thermally activated capture and emission time constants. The energy axis is obtained by adding the vibronic energy of the trap to the electron energy—note that the electron can be either free or bound when drawing an oscillator potential. The "*A*" curve represents the occupied ground state of the trap. Curve "*B*" represents the ionized trap at an electronic energy equal to the Fermi level in the metal. The "*C*" curve is drawn for the case of ionized trap and the electron at the bottom of the silicon conduction band.

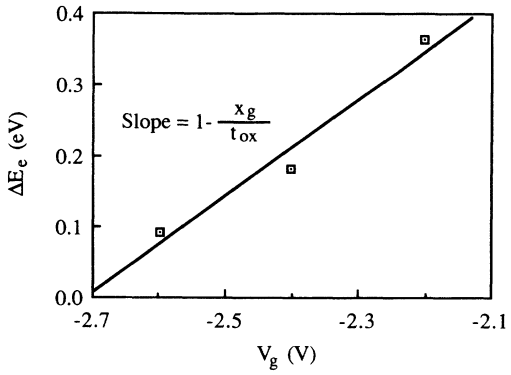

FIG. 10. Voltage dependence of the activation energy for emission from the ground state.

is the voltage-dependent activation energy, which is obtained from an Arrhenius plot of τ_e versus the temperature T. This is repeated for each gate voltage, and then the position in the x direction of the ground state, x_g, together with the activation energy at zero bias, $\Delta E_{0,e}$, is obtained using Eq. (15), as shown in Fig. 10. The position of the ground state in Fig. 7, where $x_g = 7.2$ Å and $\Delta E_{0,e} = 1.84$ eV, was deduced in this way. The preexponential factor $\tau_{0,e}$ in Eq. (14) contains the cross section for the combined thermal emission and tunneling from the ground state to the silicon.

The mean time in the high-current mode, τ_c, is also thermally activated at higher temperatures. We interpret this fact as a manifestation of the presence of relaxation phenomena[20] in association with the change in charge state upon capture and emission. When an electron is to be captured to the ground state, i.e., from "*B*" to "*A*" in Fig. 9, the empty trap must be in a certain atomic vibration mode. We further deduce that this effect is smaller when capture occurs to the excited state. If this were not so, the tunnel time constant τ_t, and thus ΔI, would also be thermally activated, which they do not seem to be, as pointed out in Sec. III. One should bear in mind that configuration-coordinate diagrams are schematically drawn along some generalized coordinate, which in general does not have a simple relationship to the Cartesian coordinates of the trap.[21] This means that the voltage dependence of the activation energy for capture to the ground state, ΔE_c, depends on the exact curvatures (in generalized coordinates) and positions of the curves "*A*" and "*B*" in Fig. 9. Unfortunately, our electric measurements cannot provide that kind of detailed information. We simply conclude that the increase in τ_c with more negative gate voltage at higher temperatures indicates an increasing energy difference ΔE_c between the bottom of the empty-trap curve "*B*" and its crossing point with "*A*" as the metal becomes more negative. This is to be expected if the equilibrium position of the trap is shifted towards the metal on ionization.

The saturation of τ_c at lower temperatures, clearly seen in Fig. 5, can be explained by a local temperature increase at the trap site due to extra power dissipation during the high-current time intervals. To give a rough estimate of the local current density in the vicinity of the trap, we assume that the trap-assisted tunnel current exits the oxide within a square whose sides are equal to the oxide thickness.[10] Choosing 20 pA for ΔI as a common value, the local current density would then be of the order 10^2 A/cm^2. With a gate voltage of -2.5 V, the locally dissipated power density would then be of the order 10^2 W/cm^2. This value may be expected to produce an amount of excess heat large enough to cause the proposed temperature increase. The more negative that gate voltage, the larger the local current ΔI, implying that more heat is dissipated locally and thus saturation occurs at a higher temperature (Fig. 5).

An alternative explanation of the fact that τ_c saturates would be that capture can occur without a thermal activation process, e.g., via direct tunneling from states in the metal well below the Fermi level, parallel to the thermally activated capture. In fact, a curve like the "*B*" curve (Fig. 9) can be drawn for any electron energy below the metal Fermi energy, resulting in a quasicontinuous set of curves. It is possible that for at least one such curve, the corresponding thermal activation energy for capture, ΔE_c, is negligibly small. The resulting direct tunneling can have a large time constant, if the coupling between the wave functions of the electron at the deep energy in the metal and the ground state of the trap is weak. This process would be present at all temperatures, but at higher temperatures the thermally activated capture would dominate and serve to decrease τ_c, because the most rapid of the two time constants would determine the total time constant.

The curvature in the temperature dependence of τ_e in Fig. 6 cannot be accounted for by the same effect of local heating as can the τ_c data, since according to our model the current density in the immediate vicinity of the trap is now equal to the lower background level. This current

density is typically several orders of magnitude lower than the local current density mentioned above, as shown in Fig. 3, and the risk of heating is small. The straightforward explanation of the phenomenon is then that there are two concurrent activation energies involved in the emission from the ground state. As shown in Fig. 7, the ground state is situated below the conduction-band edge of the silicon. Thus, it is possible that an electron leaving the ground state can reach either the silicon conduction band via thermal emission, or alternatively a hole is captured to the trap from the valence band of the silicon. The latter process can also be thermally activated in a process similar to the capture of an electron to the ground state, shown in Fig. 9, i.e., as a result of a configuration shift of the equilibrium position of the trap as the hole is captured. Which of the two processes is dominant at a given temperature is then determined by a number of parameters, and of these the difference in activation energy is very important.

V. DISCUSSION

The mechanism controlling the TLF's, as proposed in this paper, relies on a two-step tunnel process across a trap center, where an excited state serves as the current path. A transition to the ground state blocks the current for as long as the state remains occupied by the electron. The time durations of the two current levels are determined by the transition time constants of electrons to and from the ground state. Due to lattice relaxation effects these two time constants are thermally activated, which makes them about 8 orders of magnitude larger than the corresponding time constants of the excited state.

The tunnel calculation presented in Sec. IV B is to be considered as an estimate demonstrating the realism of the model, which explains the magnitude and voltage dependence of ΔI to a reasonable degree. From Fig. 4, it is seen that a more linear dependence is predicted of ΔI on V_g than we measure. A possible explanation is that stronger selection rules than implied in Eq. (12) apply for the transitions between the excited state and the Si conduction band when close to the band edge. If the wavelength of the tunneling electron becomes larger than the tunneling distance, the WKB approximation used may not be valid.

All the effects present in Figs. 2, 4, 5, and 6 can be explained in our model. The only fitted parameters in Fig. 4 are the trap distance from the metal and the energy distance between the unperturbed oxide conduction band and the excited state (Fig. 7). The other parameters of the ΔI calculation are taken either from known data of the system or are measured independently.

We have also observed more complex behaviors of the time traces, similar to the results obtained by Farmer *et al.*,[8] than simple independent TLF's. These authors conclude that the complex effects are due to strong ionic interactions between clusters of localized states. While our model does not incorporate such effects, which are extremely difficult to quantify, the existence of interaction between several traps is in principle not excluded.

ACKNOWLEDGMENTS

This work was sponsored by a grant from the Swedish National Board for Technical Development. The authors wish to thank Professor Christer Svensson at the Linköping University, Sweden, for helpful discussions.

[1]K. S. Ralls, W. J. Skocpol, L. D. Jackel, R. E. Howard, L. A. Fetter, R. W. Epworth, and D. M. Tennant, Phys. Rev. Lett. **52**, 228 (1984).
[2]M. J. Uren, D. J. Day, and M. J. Kirton, Appl. Phys. Lett. **47**, 1195 (1985).
[3]A. Karwath and M. Schulz, Appl. Phys. Lett. **52**, 634 (1988).
[4]K. Kandiah and F. B. Whiting, Solid State Electron. **21**, 1079 (1978).
[5]M. J. Kirton and M. J. Uren, Adv. Phys. **38**, 367 (1989).
[6]C. T. Rogers and R. A. Buhrman, Phys. Rev. Lett. **53**, 1272 (1984).
[7]C. T. Rogers and R. A. Buhrman, Phys. Rev. Lett. **55**, 859 (1985).
[8]K. R. Farmer, C. T. Rogers, and R. A. Buhrman, Phys. Rev. Lett. **58**, 2255 (1987).
[9]K. R. Farmer, R. Saletti, and R. A. Buhrman, Appl. Phys. Lett. **52**, 1749 (1988).
[10]F. W. Schmidlin, J. Appl. Phys. **37**, 2823 (1966).
[11]R. Stratton, J. Phys. Chem. Solids **23**, 1177 (1962).
[12]M. A. Green, F. D. King, and J. Shewchun, Solid State Electron. **17**, 551 (1974).
[13]J. Maserjian, in *Physics and Chemistry of SiO_2 and the Si-SiO_2 Interface,* edited by C. R. Helms and B. Deal (Pergamon, New York, 1988).
[14]Z. A. Weinberg, J. Appl. Phys. **53**, 5052 (1982).
[15]Z. A. Weinberg and A. Hartstein, Solid State Commun. **20**, 179 (1976).
[16]J. Maserjian, J. Vac. Sci. Technol. **11**, 996 (1974).
[17]G. Lucovsky, Solid State Commun. **3**, 299 (1965).
[18]I. Lundström and C. Svensson, J. Appl. Phys. **43**, 5045 (1972).
[19]J. Bardeen, Phys. Rev. Lett. **6**, 57 (1961).
[20]C. H. Henry and D. V. Lang, Phys. Rev. B **15**, 989 (1977).
[21]D. L. Dexter, in *Solid State Physics,* edited by F. Seitz and D. Turnbull (Academic, New York, 1958), Vol. 6.